Cell Reports, Volume *43*

Supplemental information

Pten regulates endocytic trafficking of cell adhesion and Wnt signaling molecules to pattern the retina

Yacine Touahri, Joseph Hanna, Nobuhiko Tachibana, Satoshi Okawa, Hedy Liu, Luke Ajay David, Thomas Olender, Lakshmy Vasan, Alissa Pak, Dhruv Nimesh Mehta, Vorapin Chinchalongporn, Anjali Balakrishnan, Robert Cantrup, Rajiv Dixit, Pierre Mattar, Fermisk Saleh, Yaroslav Ilnytskyy, Monzur Murshed, Paul E. Mains, Igor Kovalchuk, Julie L. Lefebvre, Hon S. Leong, Michel Cayouette, Chao Wang, Antonio del Sol, Marjorie Brand, Benjamin E. Reese, and Carol Schuurmans

SUPPLEMENTAL INFORMATION

Supplementary Figure 1. Characterizing gene expression in the P7 retinas.

(A) Dot plot of genes used to assign cellular identities to clusters in the UMAP plots of P7 retinal cells, including markers of rod photoreceptors (*Nr2e3, Nrl, Rho*), cone photoreceptors (*Arr3, Opn1mw, Opn1sw*), bipolar cells (*Vsx2, Otx2, Grm6*), Müller glia (*Sox9, Vim, Rlbp1, Plagl1*), amacrine cells (*Slc32a1, Pax6, Slc6a9, Gad2*), microglia (*Cx3cr1, Mpeg1*), endothelial cells (*Tie1, Tek, Pecam1*), pericytes (*Kcnj8, Pdgfrb*), and RPE (*Tyr, Pmel, Rpe65*). scRNA-seq was performed on 3 individual P7 wild-type retinas (SC6, 7, 8).

(B) RNAscope in situ hybridization of P7 retinas, showing co-labeling of *Dscam, Pten* and *Th*. High magnification images of single cells to the right show transcripts for *Dscam, Pten* and *Th* are located in the same cell. Blue is DAPI counterstain.

gcl, ganglion cell layer; inl, inner nuclear layer; onl, outer nuclear layer. Scale Bars: 50μm in first four panels; 10μm in high magnification images.

Supplementary Figure 2. Analysis of retinas from *Dscam*^{del17} and *Pten*^{cKO}*;Dscam*^{del17} double heterozygous intercrosses.

(A) 56 litters from *Pten*$^{fl/+}$*;Dscam*$^{+/del17}$ female with *Pten*$^{fl/+}$*; Pax::Cre*$^{+}$*;Dscam*$^{+/del17}$ male intercrosses were analysed for a total of 376 live P14 pups. Graph compares the theoretical birth rates of each genotype (black bars) to experimental birth rates (grey bars). Asterisks indicate the genotypes with lower experimental versus theoretical birth rates.

(B,C) DAPI staining of transverse sections through the retinas of P7 wild-type, *Pten* ^{cKO}, *Dscam*^{del17} and *Pten*^{cKO}*;Dscam*^{del17} retinas (B) and their measured thicknesses. Plot shows means ± SEM. N=3 biological replicates per genotype, each with 3 technical replicates. p-values calculated with one way ANOVA and post-hoc Tukey test.

(D-F) Immunolabeling of P14 wild-type, *Pten*^{cKO}, *Dscam*^{del17}, and *Pten*^{cKO}*;Dscam*^{del17} retinas with Pax6 (D), Calretinin (E), and ChAT (F).

gcl, ganglion cell layer; inl, inner nuclear layer; onl, outer nuclear layer. Scale Bar: 50μm in B, 200 μm D, E, F.

Supplementary Figure 3. Irregular SAC mosaics in *Pten*^{cKO} retinas at P7 and P21.

(A-B) Immunolabeling of P7 wild-type (A) and *Pten*^{cKO} (B) retinal flatmounts for Isl1. Voronoi tessellation and Voronoi areas depicting the distribution of Isl1^{+} amacrine cells. Nearest neighbors and frequency distributions of nearest neighbor distances of Isl1^{+} reference cells are shown. Voronoi domain and Nearest Neighbor regularity indices are plotted for wild-type and *Pten*^{cKO} retinas. Plots show means ± SEM. N=3 biological replicates per genotype, each with 4 technical replicates. p-values calculated with unpaired t test.

(C,D) Immunolabeling of P21 wild-type (C) and *Pten*^{cKO} (D) retinal flatmounts for ChAT. Voronoi tessellation and Voronoi areas depicting the distribution of ChAT^{+} amacrine cells. Nearest neighbors and frequency distributions of nearest neighbor distances of ChAT^{+} reference cells are shown. Voronoi domain and Nearest Neighbor regularity indices are plotted for wild-type and

Pten^{cKO} retinas. Plots show means ± SEM. N=3 biological replicates per genotype, each with 4 technical replicates. p-values calculated with unpaired t-test. Scale Bar: 200μm.

Supplementary Figure 4. DSCAM protein accumulates aberrantly in TH^{+} dopaminergic amacrine cells in *Pten*^{cKO} retinas.

(A) Immunolabeling of P21 wild-type, *Pten*^{cKO} and *Dscam*^{del17} retinal flatmounts with TH. Arrowheads point to TH^{+} amacrine cell process fasciculation.

(B) Colabeling of P21 wild-type and *Pten*^{cKO} retinas with TH (red) and DSCAM (green).

(C) Quantification of DSCAM^{+} puncta within individual TH^{+} cells in P21 wild-type and *Pten*^{cKO} retinal flatmounts. Plots show means ± SEM. N=4 biological replicates per genotype. A total of 138 wild-type and 177 *Pten*^{cKO} TH+ cells were evaluated. p-values above the bars were calculated with unpaired t tests for pairwise comparisons of wild-type and *Pten*^{cKO} TH^{+} cells with each puncta number. To test whether the proportions of DSCAM puncta between wild-type and *Pten*^{cKO} TH^{+} cells were different, a G-test was applied.

(D-G) Colabeling of P21 wild-type retinas with DSCAM (red) and TH (green) along with the following cell type markers: CD63 (D), γ-tubulin (E), acetyl-tubulin (F) and cholera toxin B (G). Scale Bar: 20μm in A, 5μm in B-G.

Supplementary Figure 5. Treatment of E18.5 retinal explants with bpV(pic) phenocopies the amacrine cell disruption observed in *Pten*^{cKO} retinas.

E18.5 retinal explants were treated with PBS (control) or 10μm bpV(pic) for 8 DIV. Sections were immunolabeled with Pax6. gcl, ganglion cell layer; inl, inner nuclear layer; onl, outer nuclear layer. Scale Bar: 30μm.

Supplementary Figure 6. Retinal cells secrete extracellular vesicles containing CAMs.

(A) Schematic of cell showing endosomes, multi-vesicular bodies (MVB) and secreted EVs and microvesicles.

(B) Transmission Electron Microscopy (TEM) of EVs purified from P21 wild-type retina. Scale bar: 200nm.

(C) Western blot analyses of MEGF10, Flotillin-1, TSG101 and β-actin on EVs isolated from P14 wild-type and *Pten*^{cKO} retinal EVs. Plot shows means ± SEM. N=3 biological replicates per sample from one experiment. P-values calculated with unpaired t-test.

(D) Nanoflow quantification of EVs extracted form P14 wild-type and *Pten*^{cKO} retinas. Plot shows means ± SEM. N=6 wild-type, N=5 *Pten*^{cKO} retinas from one experiment. P-values calculated with unpaired t-test.

(E) Nanoflow analysis of CD9-labeled EVs from P12 MACS-enriched amacrine cells. Plot shows means ± SEM. N=2 from one experiment.

(F) RNAscope analysis of *Pax6* (green), *Smpd3* (white) and *Pten* (red) expression in P21 retinas. Blue is DAPI counterstain. Scale Bar: 75μm.

(G) Immunolabeling of adult wild-type and *Smpd3*$^{fro/fro}$+*Col1A1* transgene (to rescue bone defects) flatmount retinas with ChAT and TH. Scale Bar: 200μm.

(H) Western blot of DSCAM and TSG101 in EVs isolated from P7 wild-type and *Pten*^{cKO} EVs, showing densitometry analyses. Plot shows means ± SEM. N=3 biological replicates per sample from one experiment. P-values calculated with unpaired t-test.

Supplementary Figure 7. Altering Wnt signaling perturbs amacrine cell positioning.

(A) β-catenin immunolabeling of P7 wild-type and *Pten*^{cKO} retinas. Scale Bar: 100μm.

(B) Treatment of P0 retinal explants with DMSO or XAV939 for 7 DIV, followed by immunostaining with Pax6. Scale Bar: 50μm.

(C) β-catenin expression in P14 wild-type and *Ctnnb1*^{cKO} retinas, confirming *Ctnnb1* deletion. Scale Bar: 50μm.

(D) Electroporation of E18.5 retinal explants with pCIG2 (control) and pCIG2-*Wnt3a* expression vectors, analysed after 8 DIV. Sections were co-immunolabeled with GFP (transfected cells) and Pax6 (amacrine cells). Scale Bar: 75μm.

(E-G) Immunolabeling P14 wild-type and *Ctnnb1*^{cKO} retinas with ChAT (E), TFAP2A (F) and PPP1R17 (G). Quantification of labeled cells in the individual layers. Plots show means ± SEM. N=3 biological replicates per genotype, each with 3 technical replicates. p-values calculated with unpaired t-test. Scale Bar: 50μm.

gcl, ganglion cell layer; inl, inner nuclear layer; ipl, inner plexiform layer; onl, outer nuclear layer.

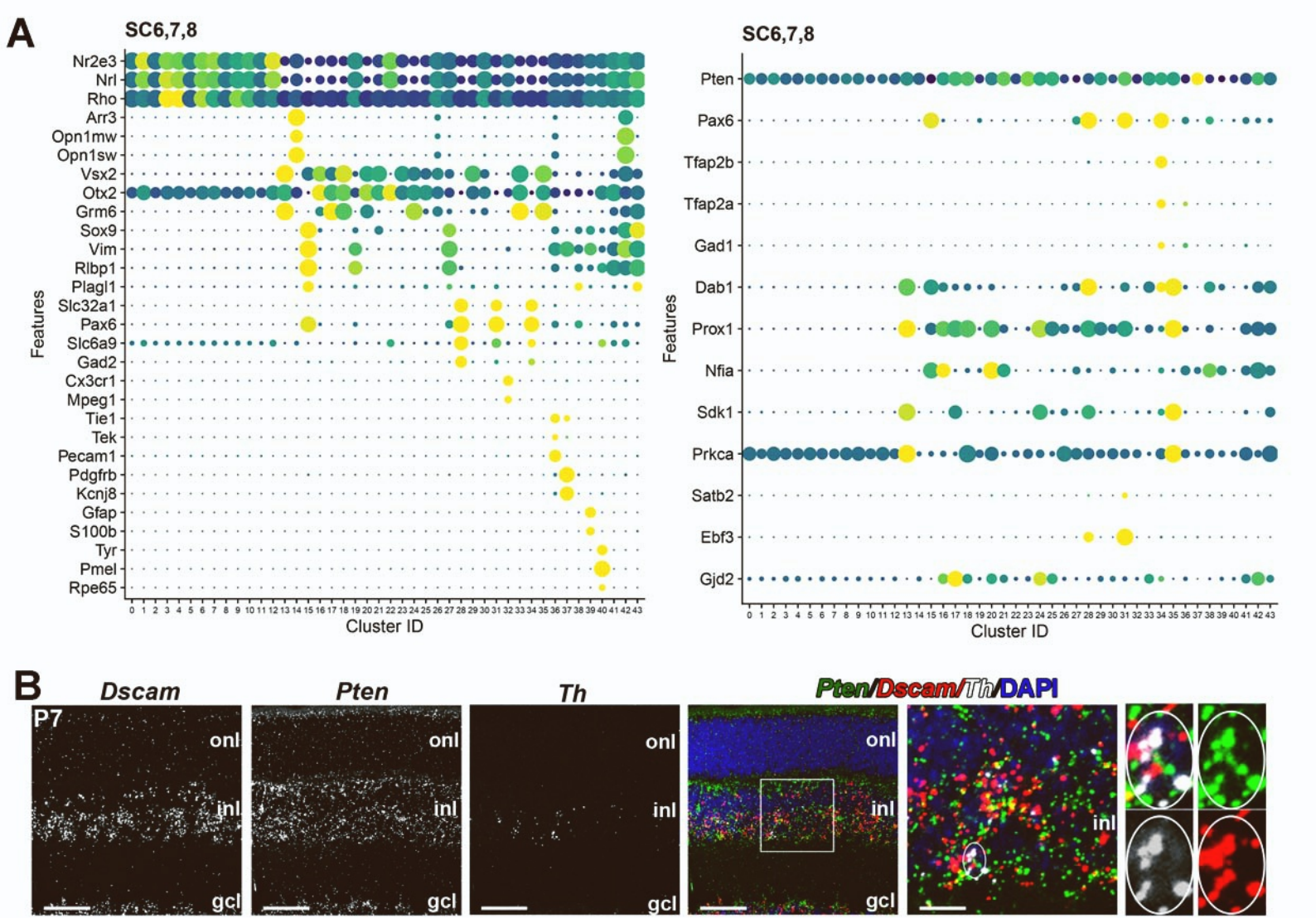

Touahri et al. Suppl. Figure 1

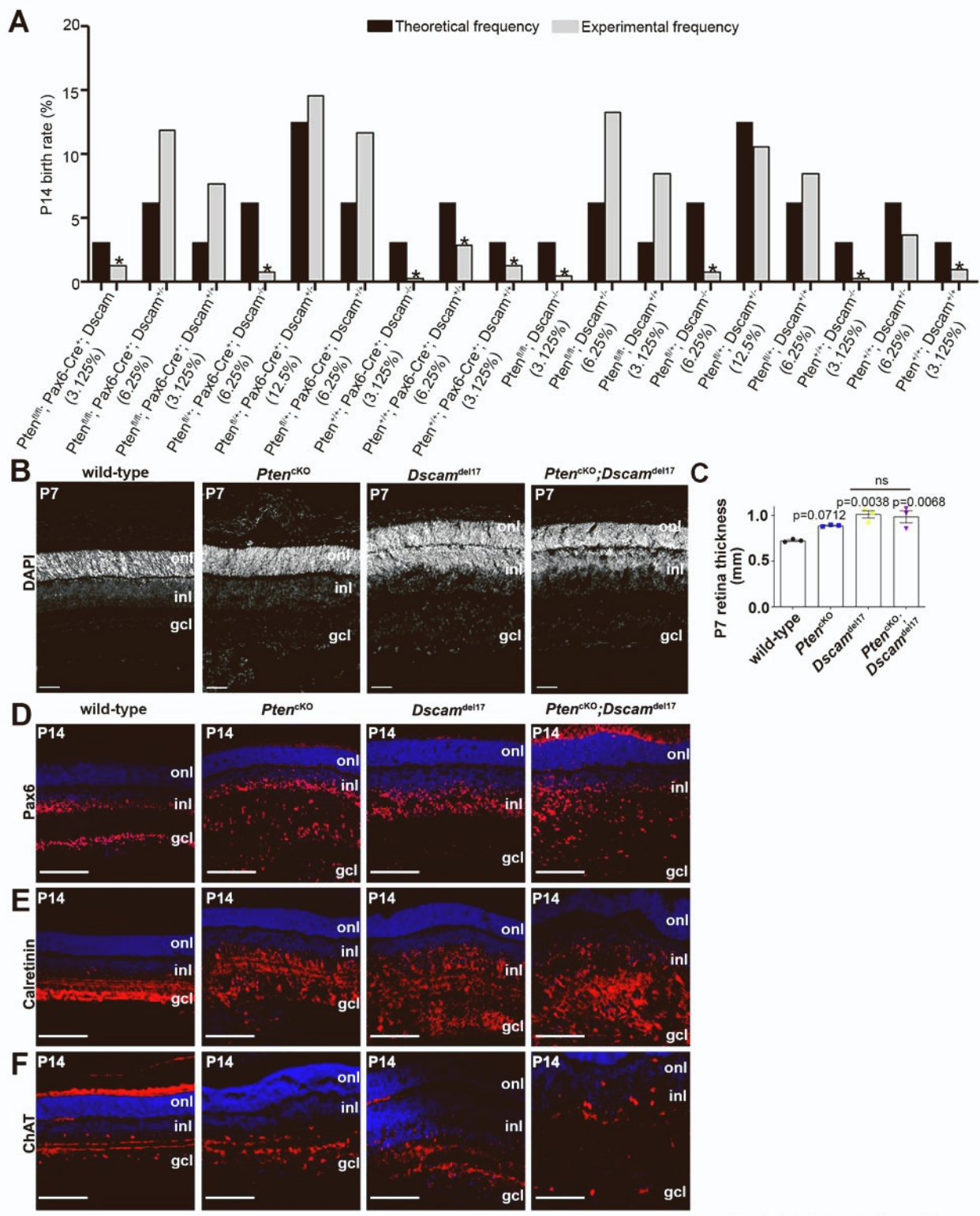

Touahri et al. Suppl. Figure 2

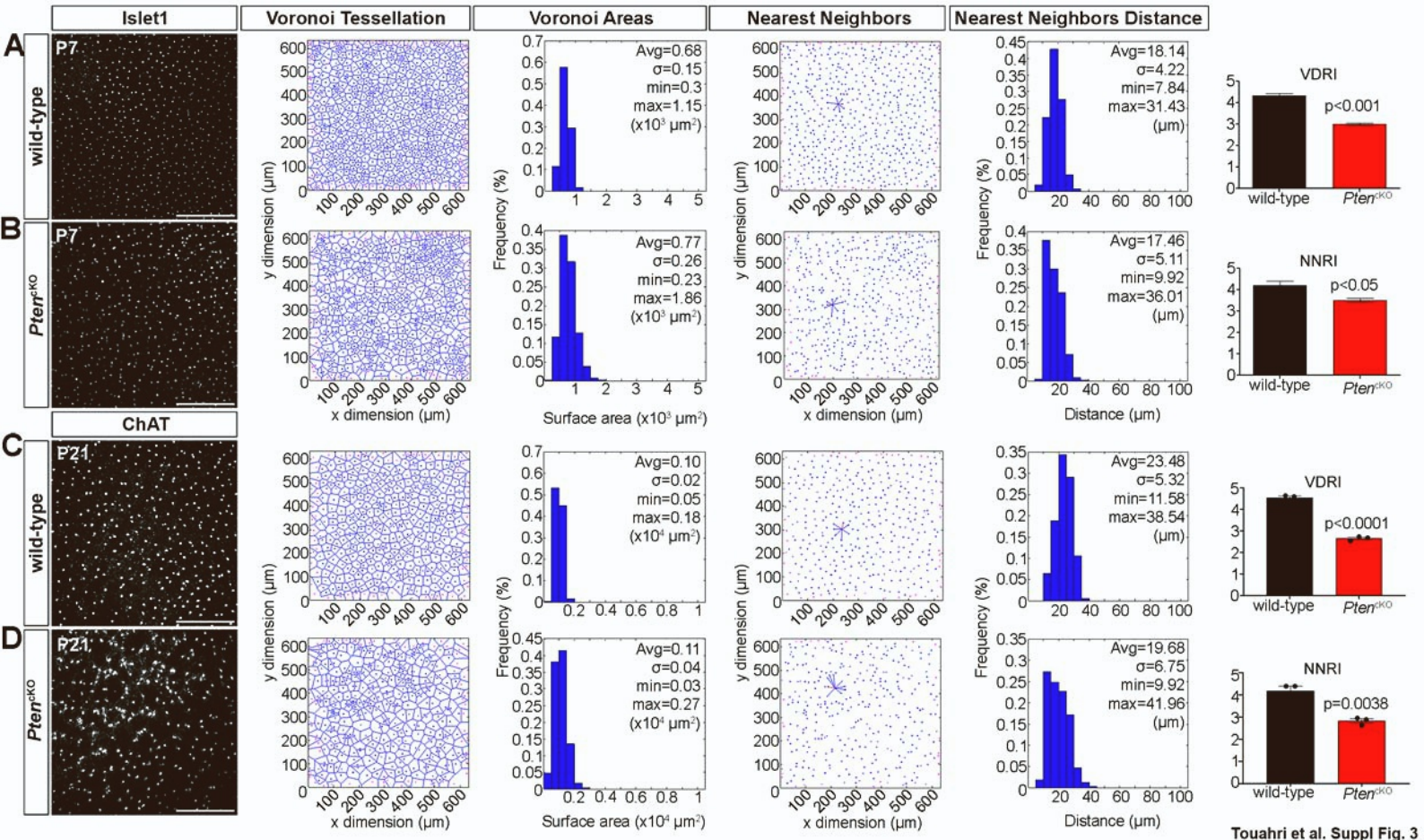

Touahri et al. Suppl Fig. 3

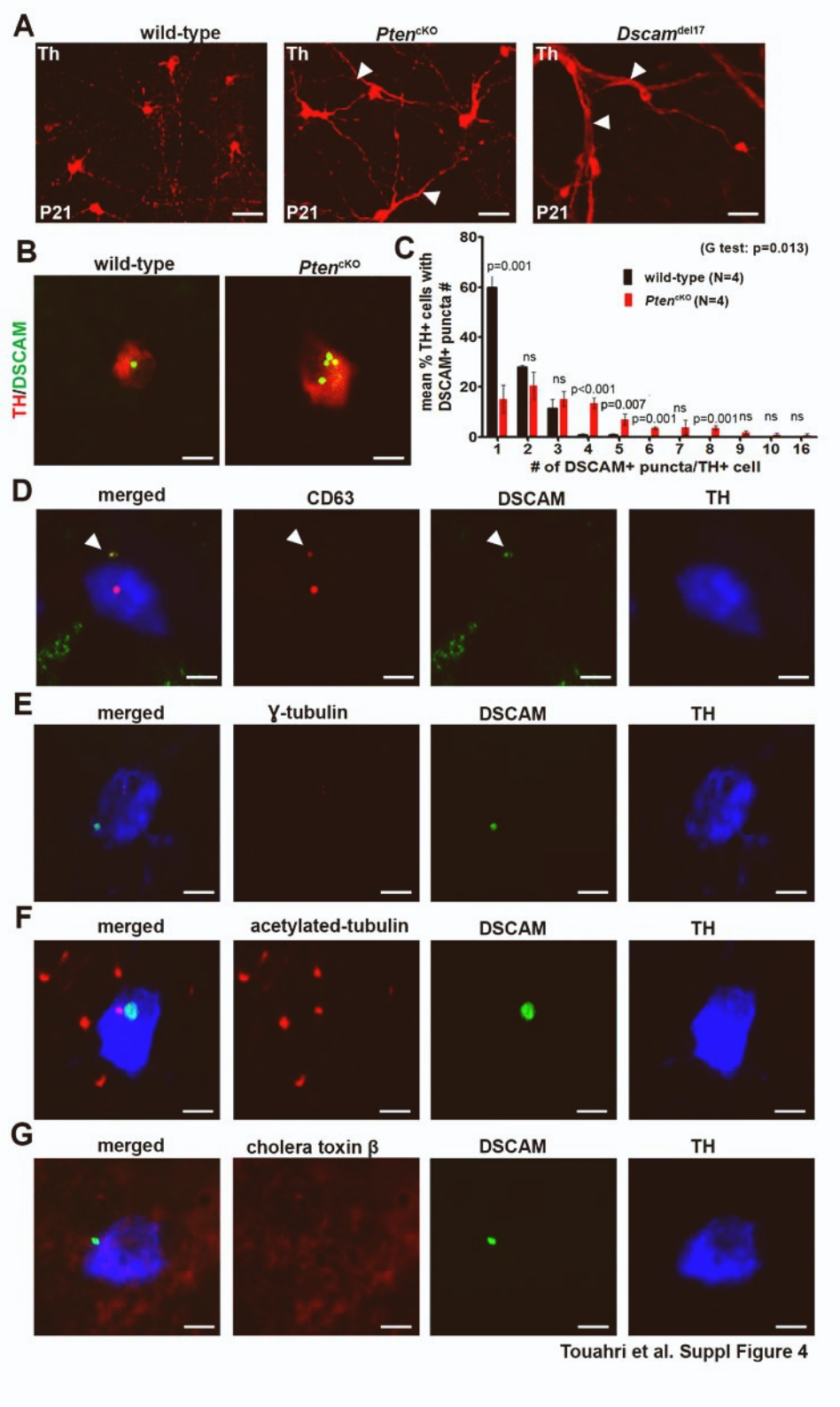

Touahri et al. Suppl Figure 4

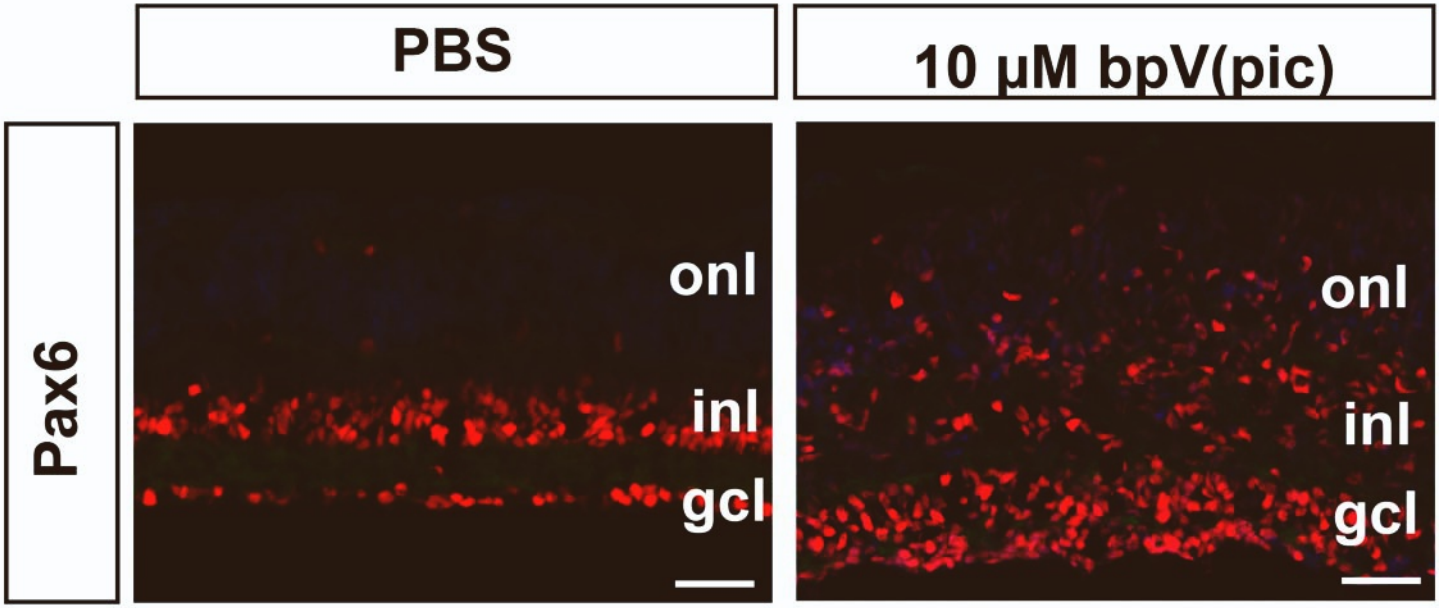

Touahri et al. Suppl. Figure 5

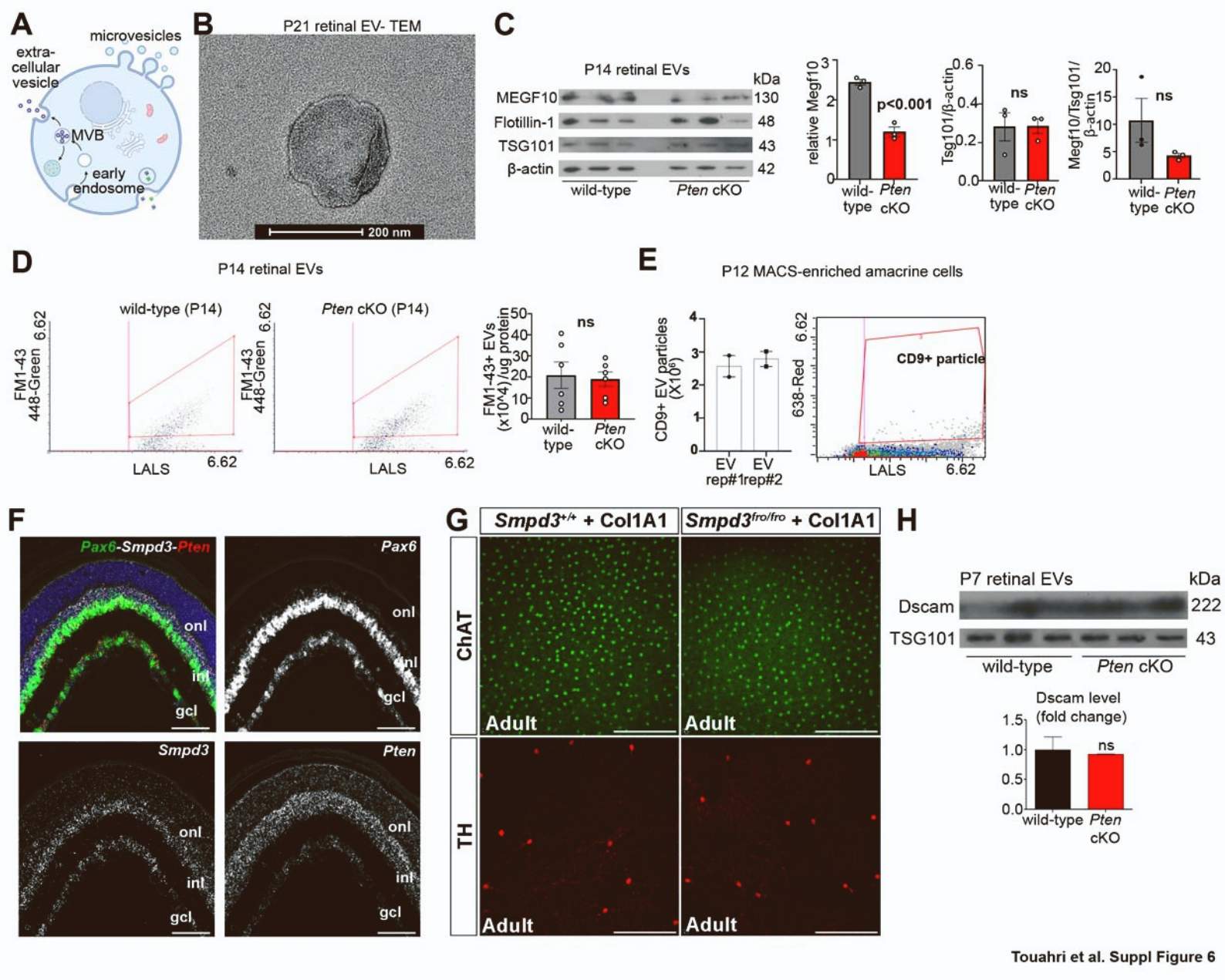

Touahri et al. Suppl Figure 6

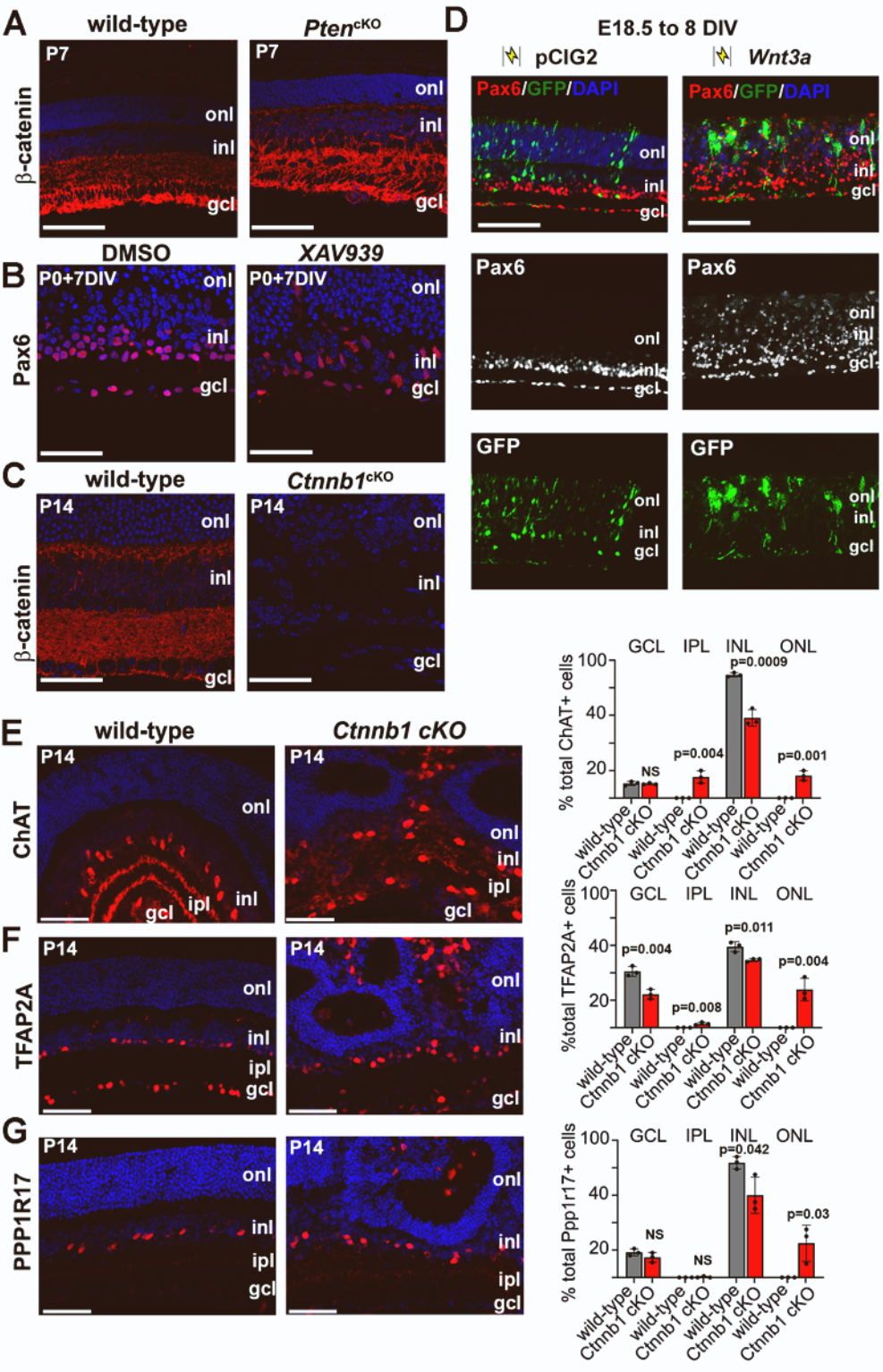

Touahri et al. Suppl Figure 7